







RESEARCH ARTICLE | SEPTEMBER 03 2024

## Experimental studies of spiral wave teleportation in a light sensitive Belousov–Zhabotinsky system

Shannyn A. Tyler ; David Mersing ; Flavio H. Fenton ; Mark R. Tinsley  ; Kenneth Showalter 



Chaos 34, 093106 (2024)

<https://doi.org/10.1063/5.0216649>



### Articles You May Be Interested In

Quint points lattice in a driven Belousov–Zhabotinsky reaction model

*Chaos* (May 2021)

Photochemical motion control of surface active Belousov–Zhabotinsky droplets

*Chaos* (August 2020)

Nonlinear effects of electric fields in the Belousov-Zhabotinsky reaction dissolved in a microemulsion

*Chaos* (April 2015)



**Chaos**

**Special Topics Open  
for Submissions**

[Learn More](#)

# Experimental studies of spiral wave teleportation in a light sensitive Belousov–Zhabotinsky system

Cite as: Chaos 34, 093106 (2024); doi: 10.1063/5.0216649

Submitted: 30 April 2024 · Accepted: 12 August 2024 ·

Published Online: 3 September 2024



View Online



Export Citation



CrossMark

Shannyn A. Tyler,<sup>1</sup>  David Mersing,<sup>1</sup>  Flavio H. Fenton,<sup>2</sup>  Mark R. Tinsley,<sup>1,a)</sup>  and Kenneth Showalter<sup>1</sup> 

## AFFILIATIONS

<sup>1</sup>Eugene Bennett Department of Chemistry, West Virginia University, Morgantown, West Virginia 26506, USA

<sup>2</sup>School of Physics, Georgia Institute of Technology, Atlanta, Georgia 30332, USA

<sup>a)</sup>Author to whom correspondence should be addressed: [mark.tinsley@mail.wvu.edu](mailto:mark.tinsley@mail.wvu.edu)

## ABSTRACT

Cardiac arrhythmias are a form of heart disease that contributes toward making heart disease a significant cause of death globally. Irregular rhythms associated with cardiac arrhythmias are thought to arise due to singularities in the heart tissue that generate reentrant waves in the underlying excitable medium. A normal approach to removing such singularities is to apply a high voltage electric shock, which effectively resets the phase of the cardiac cells. A concern with the use of this defibrillation technique is that the high-energy shock can cause lasting damage to the heart tissue. Various theoretical works have investigated lower-energy alternatives to defibrillation. In this work, we demonstrate the effectiveness of a low-energy defibrillation method in an experimental 2D Belousov–Zhabotinsky (BZ) system. When implemented as a 2D spatial reaction, the BZ reaction serves as an effective analog of general excitable media and supports regular and reentrant wave activity. The defibrillation technique employed involves targeted low-energy perturbations that can be used to “teleport” and/or annihilate singularities present in the excitable BZ medium.

Published under an exclusive license by AIP Publishing. <https://doi.org/10.1063/5.0216649>

Cardiac arrhythmias are associated with spatiotemporal irregularities in the heart’s electrical activity.<sup>1,2</sup> They reduce the heart’s ability to pump blood and can lead to sudden cardiac arrest.<sup>3,4</sup> While their origin is complex, they are associated with reentrant waves generated by singularities in the activity of the heart tissue.<sup>5</sup> A standard defibrillation approach is the application of a high-energy electrical stimulus. This effectively resets the phase of the electrical activity in the tissue and restores regular oscillatory behavior.<sup>6</sup> A concern with this defibrillation method is that it can lead to lasting damage to the heart tissue.<sup>7</sup> Recently, a low-energy defibrillation technique was proposed.<sup>8</sup> The study showed the possibility of instantaneously relocating the position of a spiral wave tip (this is termed “teleportation”) to any point in space using a precisely tailored stimulus derived from phase space information. Of particular note is the ability of the technique to instantaneously shift all spiral waves within a domain to their counterparts, leading to their immediate elimination with a minimal stimulus. In the current work, we use experiments on spiral waves in the photosensitive BZ reaction to demonstrate singularity teleportation and elimination using this

minimal stimulus.<sup>9,10</sup> This paves the way for its application in biological systems that support spiral waves such as the heart and the brain.

## INTRODUCTION

Heart disease, encompassing various conditions affecting the heart, remains the leading cause of death globally.<sup>1,2</sup> Among the numerous complications associated with heart disease, cardiac arrhythmias stand out as a significant contributor to mortality.<sup>11</sup> Cardiac arrhythmias are abnormal electrical activity in the heart that can disrupt its regular beating pattern. These electrical disturbances and alterations in the heart’s blood pumping ability can have detrimental consequences, such as stroke and sudden cardiac arrest.<sup>3,4</sup>

The precise mechanisms underlying cardiac arrhythmias are complex and not fully understood.<sup>5</sup> However, phase singularities in electrical activity such as those seen at the cores of scroll and spiral waves have emerged as key phenomena associated with the

initiation and persistence of cardiac arrhythmias.<sup>12–14</sup> These reentrant waves are characterized by rotating patterns of activity around the core singularity. They lead to complex spatiotemporal patterns of electrical activity which contribute to the characteristic fast heart rate observed in tachycardia and irregular heart rate rhythm during fibrillation.

It has long been known that termination of these fatal arrhythmias is possible using high-energy electric shocks, known as defibrillation, which resets the electrochemical activity of the heart and restores the normal heart rhythm.<sup>6</sup> Typical defibrillation shocks used in clinical practice can range in strength from 200 to 360 joules.<sup>15</sup> Although this type of defibrillation is required to ensure effective removal of reentrant wave activity, it is painful and can cause significant damage to the heart tissue.<sup>7</sup> For this reason, there have been efforts to develop alternative methods of defibrillation.<sup>16–18</sup> These approaches aim to achieve successful defibrillation while minimizing potential harmful effects associated with high-energy shocks. In a recent work, DeTal *et al.* proposed a new method for eliminating spiral waves in excitable media with minimal stimulus.<sup>8</sup> They demonstrated a novel low-energy defibrillation mechanism that can be applied to phase singularities in a theoretical 2D system.

Phase singularities are points in space and time where the phase of a propagating wave becomes undefined or exhibits a sudden change.<sup>19</sup> They are described as topological defects in wave patterns, particularly, in excitable media like cardiac tissue. Winfree and Strogatz used topological considerations to explain the dynamics of phase singularities.<sup>20</sup> They demonstrated that, under certain conditions, specific stimuli can lead to the creation of singularities while Krinsky *et al.* and Keener explored the termination of singularities.<sup>21,22</sup> Krinsky *et al.* showed that contour perturbations could initiate more spiral waves, and that in some cases, these new spirals could collide with the existing ones, extinguishing them all. They also showed that perturbations could bring spiral waves together and annihilate them. Keener showed why these stimuli could terminate spiral waves by correlating the initiated waves' fronts and backs with respect to the phase singularity in phase space. In general, singularities can only be created or destroyed in pairs of opposite chirality. This principle, often referred to as the "topological conservation law," implies that the total topological charge remains conserved during their creation or annihilation processes.<sup>20,23,24</sup> This principle does not apply when a singularity interacts with a system boundary.

DeTal *et al.* used this concept of singularities having opposite pairs of chirality in establishing their low-energy defibrillation mechanism.<sup>8</sup> By applying an excitable stimulus along the back of a particular excitability contour of a reaction-diffusion wave, a pair of singularities with opposite chirality can be connected. If the contour is continuous between the pair of singularities, the singularities rapidly terminate. If it is not, a spiral tip is teleported from one place to another. Thus, effective defibrillation is obtained when all spirals are teleported or annihilated by the merging of each singularity with another of opposite chirality.

Phase singularities also occur in other excitable media, such as the Belousov–Zhabotinsky (BZ) reaction.<sup>25</sup> The BZ reaction is commonly used as a model for natural excitable systems due to its ability to exhibit a wide range of equivalent spatiotemporal dynamics,

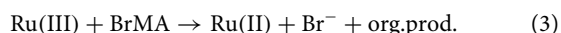
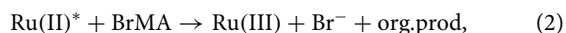
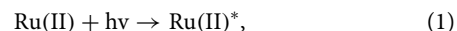
including oscillations and spatiotemporal waves.<sup>9,10</sup> The reaction involves the bromination of an acidified organic substrate in the presence of a metal catalyst. If ruthenium (II)-bipyridal is used as the metal catalyst, the reaction is then photosensitive and the phase of a given chemical oscillation can be adjusted by an appropriate perturbation in light intensity.<sup>26,27</sup>

In this work, we utilize the photosensitive BZ reaction to explore the process of low-energy defibrillation in an excitable medium. Experiments are conducted using a thin gel, which is loaded with the photosensitive catalyst that is immersed in a catalyst-free BZ solution. Following the initiation of spiral wave activity in the gel, we demonstrate that spiral tips can be teleported and/or annihilated by appropriate targeting of excitability contours using activatory light perturbations.

## EXPERIMENTAL METHODS

Experiments are carried out using the photosensitive BZ reaction, which is monitored with a computer-interfaced camera and illuminated with a computer-controlled video projector. The wave behavior is studied in a thin layer of silica gel (15% w/w) in which the photosensitive ruthenium (II)-bipyridal catalyst (5 mM) is immobilized.<sup>28–30</sup> The gel is cast onto a microscope slide and submerged in a continuously refreshed shallow catalyst-free BZ solution. The modified video projector and video camera (CCD) are interfaced with a computer allowing real-time control for perturbing the light sensitive medium and monitoring the response. The system is maintained in an excitable state with an illumination intensity of approximately  $6.0 \times 10^{-3} \text{ W m}^{-2}$ .<sup>31,32</sup> The reaction mixture composition,  $[\text{BrO}_3^-] = 0.760 \text{ M}$ ,  $[\text{malonic acid}] = 0.012 \text{ M}$ ,  $[\text{bromomalonic acid}] = 0.112 \text{ M}$ , and  $[\text{H}_2\text{SO}_4] = 0.600 \text{ M}$ , is prepared so that the system is excitable in the dark state. The border of the region of interest of the gel is illuminated with a high light intensity. This border region is then incapable of supporting wave activity.

The response of the photosensitive BZ reaction to light perturbation is dependent on the composition of the catalyst-free recipe.<sup>27</sup> Under the conditions chosen for this experiment, the dominant photochemical channel results in an increase in the production of the reaction inhibitor, bromide, following an increase in light intensity.<sup>33,34</sup> This photochemical channel can be understood through the following reaction steps:



An increase in light intensity leads to the excitation of Ru(II) ions. The excited ion is then involved in a sequence of redox reactions with bromomalonic acid (BrMA), one of the products of which is the bromide ion. Conversely, reducing the light intensity results in a decrease in the rate of this process and leads to a lowering of inhibitor production. Hence, wave activity can be initiated in the gel by reducing the projected light intensity in a region of interest, i.e., by applying a targeted dark perturbation to the gel. In general, the region of interest is the refractory back contour. This contour is

identified manually prior to each targeting as the region parallel and to the immediate rear of the region of the traveling wave of interest. A perturbation is applied for 3 s. Wave tips can be generated in the medium by using high intensity light from a laser-pointer to annihilate sections of a planar wave.

## NUMERICAL ILLUSTRATION OF UNIDIRECTIONAL WAVE INITIATION

Chemical dynamics that allow for teleportation of spiral waves and defibrillation can be explained using ideas originally developed by Winfree<sup>13,19</sup> and a 1D photosensitive model of the BZ reaction<sup>35,36</sup> (see the Appendix). Figure 1 shows the spatial profiles of the activator,  $\text{HBrO}_2$ , inhibitor,  $\text{Br}^-$ , and oxidized form of the ruthenium catalyst for a BZ reaction-diffusion wave traveling from left to right. The wave has three characteristic regions: the excited region with high activator concentration, the refractory region where the activator is decreasing and the inhibitor is high, and the recovered region where both inhibitor and activator are low. Wave initiation is not possible in the refractory region due to high inhibitor concentration. This is demonstrated in Fig. 1(i) where a dark perturbation at

point A does not result in the initiation of a wave. If a dark perturbation is applied at point C, Fig. 1(iv), in the recovered region, bidirectional wave propagation occurs with two new waves forming that propagate in opposite directions. If, however, a perturbation is applied at point B, Fig. 1(iii), on the boundary between the refractory and recovered regions, a single wave propagates into the recovered region, i.e., unidirectional wave propagation. The location of this vulnerable region, where a unidirectional wave is initiated, is dependent on both the magnitude and duration of the perturbation. It lies closer to the original propagating wave for a larger perturbation size.

## EXPERIMENTAL INITIATION OF UNIDIRECTIONAL WAVES

A 2D BZ photosensitive system, constructed using a catalyst-loaded silica gel submerged in a catalyst-free BZ solution, supports excitable reaction-diffusion waves. Appropriate choice of the catalyst-free recipe allows wave initiation using targeted perturbations in light intensity. Figure 2 (multimedia available online) shows the initiation of a unidirectional wave segment in the experimental system behind a wave traveling from right to left, Fig. 2(i). To

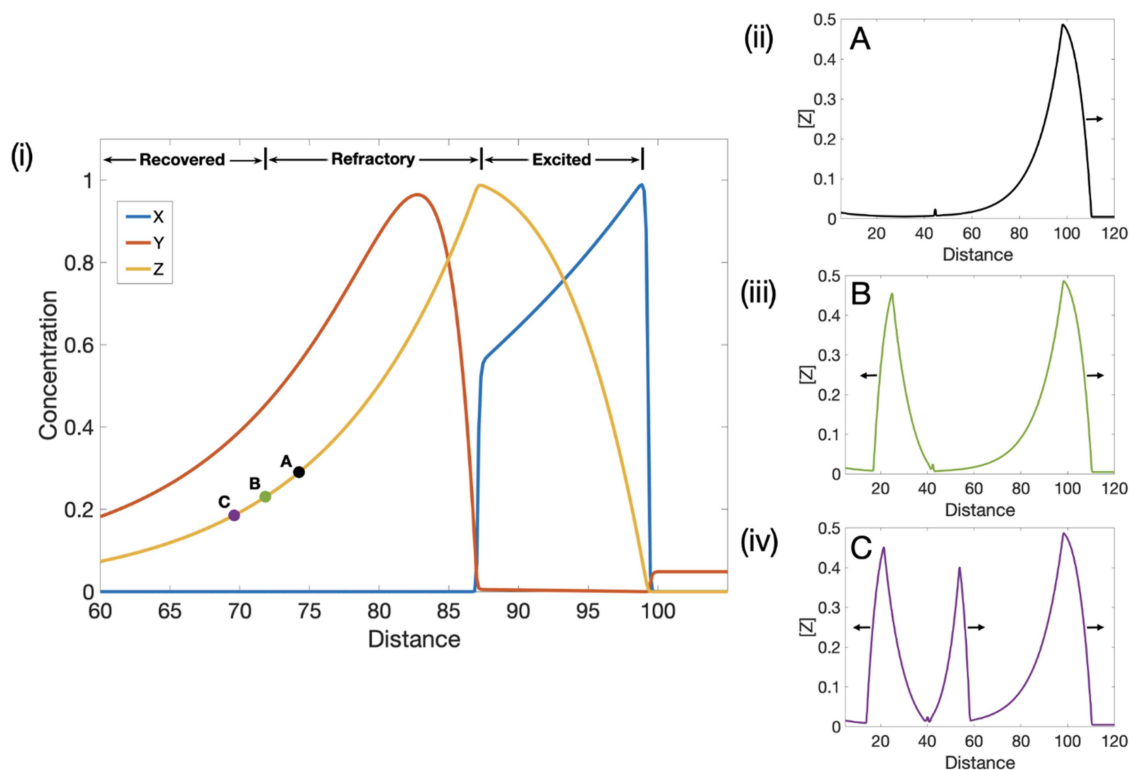


**FIG. 1.** Wave initiation in 1D simulations. (i) Spatial profiles of the scaled model variables,  $X$ ,  $Y$ , and  $Z$ . The wave is traveling from left to right. The approximate locations of the excited, refractory, and recovered regions are also shown. The response of the system to a perturbation at points A, B, and C are shown in (ii)–(iv), respectively. Point B lies on the border of these two regions. A dark perturbation applied at point A, in the refractory region, results in no wave being initiated. A dark perturbation applied at point C, in the recovered region, results in a bidirectional wave being initiated. A dark perturbation applied at point B, at the boundary between the refractory and recovered regions, results in a unidirectional wave being initiated, which then travels away from the preexisting wave (from right to left).

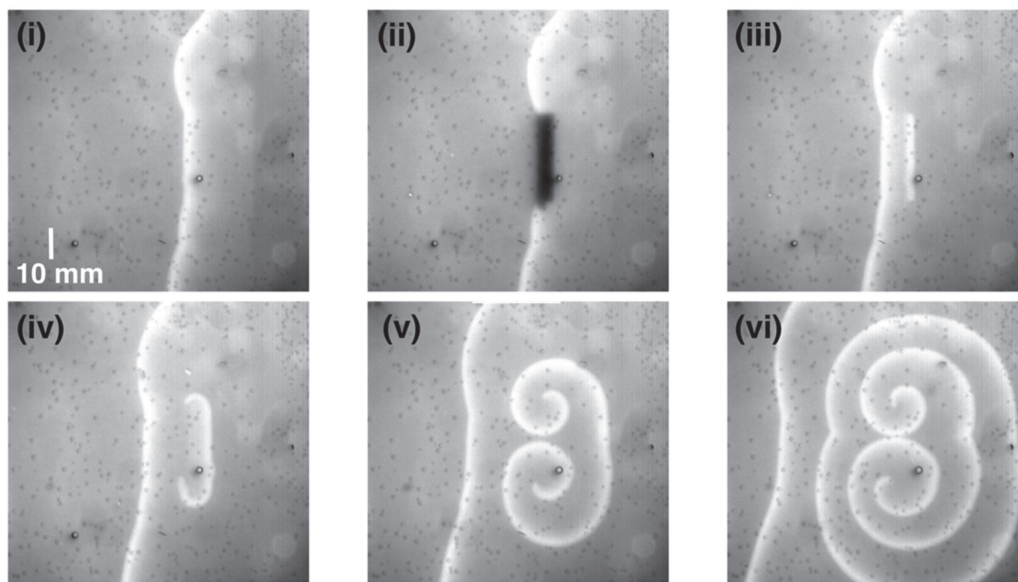


**FIG. 2.** Initiation of a wave segment. (i) A reaction-diffusion wave extends along the entire length of the excitable medium, with each end of the wave attached to a boundary. The wave travels from right to left. (ii) A dark perturbation is applied, targeting the refractory back contour. (iii) The original wave and the new wave segment initiated by the dark perturbation. The new wave travels from left to right. (iv) and (v) The newly initiated wave segment develops into a counter-rotating spiral wave pair. Images (i)–(vi) are taken at times 5, 7, 10, 15, 25, and 38 s, respectively. Multimedia available online.

achieve this, a perturbation of approximately 3 s is applied targeting a section of the refractory back contour behind the original wave, Fig. 2(ii). This contour delineates the refractory and recovered regions of the medium and is equivalent to point B, Fig. 1(i), in the simulations described above. Figure 2(iii) shows the newly formed wave segment. The free ends, or wave tips, of this wave segment are associated with discontinuities in the phase of the chemical dynamics and develop into cores of spiral wave activity, Figs. 2(iv)–2(vi).

This method of refractory back contour perturbation is similar to approaches developed by Winfree as a method of spiral wave initiation.<sup>19,37–39</sup> If, instead, a section of the refractory back contour is targeted that is continuous, or close to continuous, with one or more existing free ends (associated with either spiral cores or developing spiral cores), singularities may be teleported and/or annihilated. Following such a perturbation along a section of the refractory back contour, we observe that the new wave segment initiates in one of the two ways in the vicinity of an existing singularity. First, in a discontinuous initiation, the free end of the initiated wave segment forms close to the original singularity, rotating counter to it, and the two wave tips quickly collide and annihilate. This behavior is exhibited in the experiments associated with spiral wave teleportation, Fig. 3. Alternatively, a continuous initiation can occur. If the initiated wave segment forms spatially continuous to the original singularity, then the original wave tip is eliminated instantaneously. Examples are shown in Figs. 4 and 5. In either the continuous or discontinuous case, the initial singularity is effectively transported to the opposite end of the perturbed section of the refractory back contour. The resulting behavior is, therefore, dependent on the chosen location of this opposite end of the perturbed section.

## SPIRAL WAVE TELEPORTATION

Figure 3 (multimedia available online) shows a perturbation targeted along the refractory back contour in the vicinity of a single free end, Fig. 3(a-i), red dot. In this example, the perturbation is terminated some distance away along the refractory back contour, Fig. 3(a-ii). As seen in Fig. 3(a-iii), a new wave segment is formed. One of the wave tips associated with this new segment forms, with opposite chirality, very close to the existing wave tip and the two wave tips quickly collide and annihilate to form a continuous wave, Fig. 3(a-iv). The opposite end of the perturbed section has a phase that is abruptly different to that of the surrounding medium and a new singularity, wave tip, forms at this location, Figs. 3(a-iv)–3(a-vi). The perturbation, therefore, results in the teleportation of the original free end from its initial location, Fig. 3(a-i), red dot, to a new location, Fig. 3(a-vi), blue dot.

A spiral tip can be teleported multiple times. In Fig. 3(b), the spiral tip that was transported in Figs. 3(a) and 3(b-i), blue dot, is transported for a second time using a second perturbation targeted along the new refractory back contour. Following this second perturbation, a new wave tip of opposite chirality forms very close to the existing wave tip, Fig. 3(b-iii), and the two wave tips quickly collide and annihilate. A new wave tip forms at the opposite end of the perturbed section, Figs. 3(b-iv)–3(b-vi), with the same chirality as the original wave tip.

## SPIRAL WAVE BOUNDARY TERMINATION

If the perturbed section of the refractory back contour is terminated at the boundary of the medium, the wave tip is teleported to



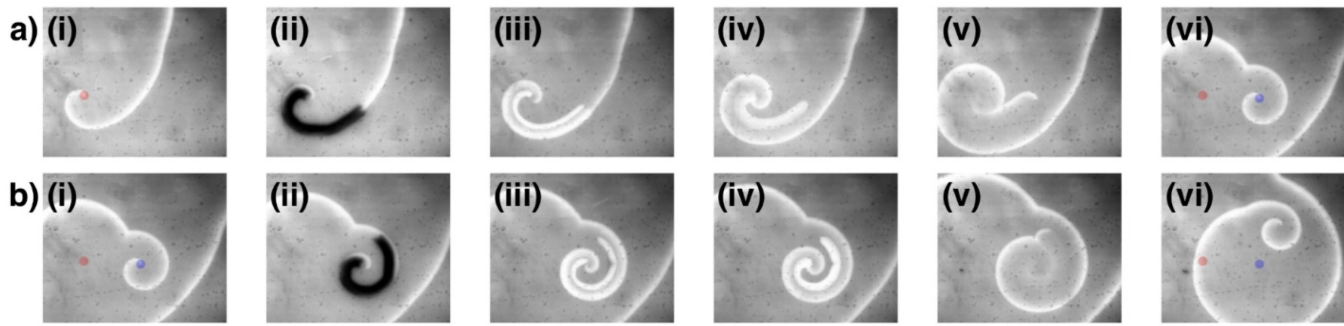


**FIG. 3.** Spiral wave tip teleportation. (a) Spiral wave tip teleportation after one perturbation and (b) spiral wave tip teleportation after a second perturbation. For each row, (i) the red and blue dots represent the locations of the original wave tip and teleported (after one perturbation) wave tip, respectively. (ii) A dark perturbation targets the refractory back contour. (iii) The original wave and the newly initiated wave segment. (iv) and (v) The original wave tip and the wave tip at one end of the new segment collide and annihilate (merge), leaving only one wave tip at the other end of the new wave segment. (vi) The spiral wave after the wave tip has been teleported. The locations of the original wave tips are indicated by red and blue dots. Images (i)–(vi) in row (a) are taken at times 5, 8, 9, 12, 17, and 28 s, respectively. Images (i)–(vi) in row (b) are taken at times 28, 31, 32, 33, 38, and 48 s, respectively. Multimedia available online.

the boundary and destroyed. This non-chirality preserving process is illustrated in Fig. 4 (multimedia available online). The refractory back contour associated with a single wave tip, Fig. 4(i), is perturbed, Fig. 4(ii), so that the opposite end of the perturbed section terminates at the boundary of the medium. In this case, since the initiated region is continuous with the original wave tip, the tip is instantaneously eliminated. The opposite end of the initiated unidirectional wave segment, Fig. 4(iii), is positioned at the high light intensity border. Since this part of the medium is not capable of supporting wave activity, the teleported singularity is destroyed. The resultant plane wave then tracks the upper edge of the medium, Figs. 4(iv) and 4(v), before it is destroyed, when it runs into the right- and left-hand side border region, Fig. 4(vi).

### SPIRAL WAVE PAIR ANNIHILATION

If a perturbation is applied so that one end of the perturbed section is in the vicinity of a wave tip and the other end is in the vicinity of another wave tip, the pair of wave tips will be eliminated. This is illustrated in Fig. 5 (multimedia available online). In Fig. 5(i), a single wave segment is initially visible in the gel medium, its two free ends having opposite chirality. A perturbation is then applied targeting the refractory back contour that joins the two wave tips, Fig. 5(ii). The initiated region forms, continuous with the original wave tips, Fig. 5(iii). This results in the effective merging of the original two wave tips and the annihilation of this spiral wave pair. An alternative perspective is that each initial wave tip is eliminated locally as the new region of wave forms. Each original wave tip is

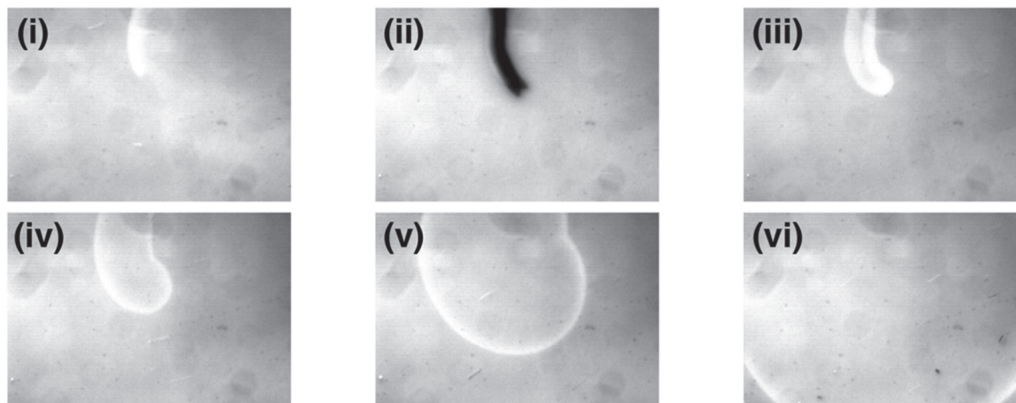


**FIG. 4.** Boundary termination of a spiral wave. (i) A wave segment with one wave tip. (ii) A dark perturbation is applied to the wave, with one edge of the perturbation touching the boundary of the excitable medium. (iii) The original wave and the newly initiated wave region. The wave tip of the newly initiated wave region forms a continuous loop with the original wave tip, terminating the original singularity. (iv)–(vi) The resultant wave loop grows outward, spreading across the medium. Images (i)–(vi) are taken at times 5, 8, 10, 15, 30, and 59 s, respectively. Multimedia available online.

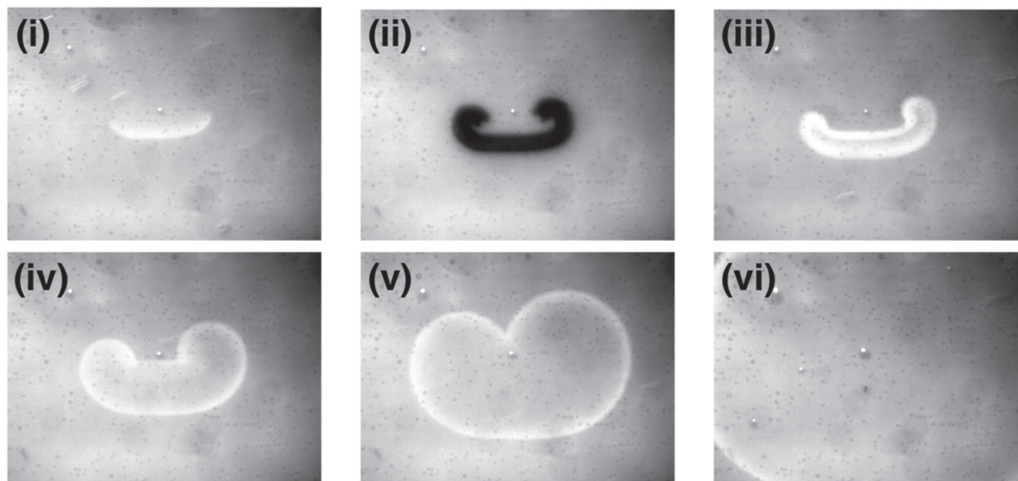


**FIG. 5.** Annihilation of counter-rotating wave tips. (i) A wave segment with two wave tips. (ii) A dark perturbation is applied targeting the refractory back contour. (iii) The original wave and the new wave region that was initiated after the perturbation. The wave tips of the newly initiated wave are continuous with the original wave, effectively annihilating the original pair of wave tips. (iv)–(vi) The resultant single wave loop grows outward spreading across the medium. Images (i)–(vi) are taken at times 5, 8, 10, 15, 24, and 50 s, respectively. Multimedia available online.

transported along the newly initiated region, where they meet and mutually annihilate. The medium now contains a single closed loop of wave activity that propagates outward to the borders of the region, Figs. 5(iii)–5(vi).

## CONCLUSION

We have presented a low-energy defibrillation technique that relies on connecting, via a common refractory back contour, opposite chiral pairs of spiral tips. Once so connected, a pair of tips effectively mutually annihilates. A single spiral tip can also be eliminated if it is connected via a dark perturbation to a boundary incapable of supporting wave activity.

The connection is created through an applied excitable perturbation along a refractory back contour. As outlined above, we have confirmed the two types of behavior theoretically predicted by DeTal *et al.*, using our experimental system following the application and the removal of the perturbation.<sup>8</sup> In the first case, a wave tip forms at the end of the new wave segment in the vicinity of the initial spiral tip. These two singularities quickly merge. In the second case, the perturbed section is observed to excite continuous to an existing spiral tip, i.e., the initiated region and the original tip merge.

While in principle these two cases are different,<sup>8</sup> in our experimental system, the second case may be an example of the first case with the merging of the pair of tips occurring before the perturbation is removed. It is not experimentally possible to visualize wave activity in the perturbed region while the perturbation is active. Regardless of this detail, the net result is the same: local elimination of the initial tip and its effective transportation along the newly formed region of wave activity.

In general, our experiments were the most successful when the perturbation was biased slightly ahead of the refractory back contour

(i.e., biased toward the excited and refractory regions, Fig. 1). This is due to the finite time necessary for a new unidirectional wave to initiate, combined with the continuous motion of the existing wave. Without this bias, the recovered region of the wave back may instead be perturbed, which results in the formation of new bidirectional waves.

A second experimental consideration is that heterogeneities within the gel medium can lead to broken initiation along the wave back resulting in the formation of two or more new wave segments. This occurs more often when the length of the perturbed section is larger and can lead to an increase in the number of wave tips. Similar increases in the number of singularities, rather than decreases, have been reported that are associated with other defibrillation techniques.<sup>40,41</sup> Using the presented technique, this issue can be alleviated by using a series of shorter length perturbations. To transport a single wave tip to a boundary, it is better to transport the tip in a series of short steps (such as in Fig. 3), and then, transport it into a border. Similar considerations should be given when attempting to mutually eliminate a pair of counter-rotating spiral tips.

After taking into account these experimental considerations, the developed technique has proven remarkably robust, particularly considering that all refractory back contour targeting was performed manually. Further to this, provided the stimulus is applied within the general vicinity of a spiral tip, the initiated tip quickly merges with it, as described earlier. This will be of particular importance if the spiral tips are meandering.<sup>42</sup> The presented work deliberately used gel media containing a low number of singularities. Future experimental work can expand this study using gel media containing more complex reentrant wave activity. Automated image analysis can be used to identify and connect paired centers. Methods adapted from the current study can then be used to algorithmically target the refractory back contours and can be applied to other systems,

in particular, to test as a low-energy anti-arrhythmic cardiac therapy. Since fibrillation can be mostly a 3D effect, effective delivery of this type of stimulation in 3D may first require studies in thin preparations.<sup>43,44</sup> For example, the current technique developed here could be directly applied in the studies of defibrillation in cardiac monolayers, especially, those created with human induced pluripotent stem cells (hiPSC) as well as in thin preparations of cardiac tissue, such as *ex vivo* atrial tissue and *ex vivo* right ventricular preparations, using optical mapping.<sup>45</sup>

## ACKNOWLEDGMENTS

This material is based on the work supported by the National Science Foundation (NSF) (Grant No. CHE-2102137) (M.R.T. and K.S.) and the National Institutes of Health (Grant No. 2R01HL143450-05A1) (F.H.F.).

## AUTHOR DECLARATIONS

### Conflict of Interest

The authors have no conflicts to disclose.

## Author Contributions

**Shannyn A. Tyler:** Conceptualization (equal); Investigation (equal); Methodology (equal); Writing – original draft (equal). **David Mersing:** Conceptualization (equal); Investigation (equal); Methodology (equal); Writing – review & editing (equal). **Flavio H. Fenton:** Conceptualization (equal); Funding acquisition (equal); Methodology (equal). **Mark R. Tinsley:** Conceptualization (equal); Funding acquisition (equal); Methodology (equal); Writing – original draft (lead). **Kenneth Showalter:** Conceptualization (equal); Funding acquisition (equal); Methodology (equal); Writing – review & editing (equal).

## DATA AVAILABILITY

The data that support the findings of this study are available from the corresponding author upon reasonable request.

## APPENDIX: COMPUTATIONAL METHODS

Simulations of spatiotemporal behavior were carried out with a three-variable Oregonator model for the photosensitive BZ reaction,<sup>46–48</sup>

$$\varepsilon \partial x / \partial t = D_x \nabla^2 x + x(1 - x) + y(q - x), \quad (\text{A1})$$

$$\varepsilon' \partial y / \partial t = D_y \nabla^2 y + fz - y(q + x) + \phi, \quad (\text{A2})$$

$$\partial z / \partial t = D_z \nabla^2 z + x - z + \phi/2, \quad (\text{A3})$$

where  $x$ ,  $y$ , and  $z$  represent the dimensionless concentrations of bromous acid, bromide, and the oxidized form of the catalyst, respectively.  $D_x$ ,  $D_y$ , and  $D_z$  are diffusion coefficients for the activator ( $\text{HBrO}_2$ ), the inhibitor ( $\text{Br}^-$ ), and the oxidized catalyst ( $[\text{Ru}(\text{bpy})_3]^{3+}$ ), respectively. Because the  $\text{Ru}(\text{III})$  complex is immobilized in the silica gel, the corresponding diffusion coefficient  $D_z = 0$ , while  $D_x = D_y = 1.0$ .  $\varepsilon$ ,  $\varepsilon'$ ,  $f$ , and  $q$  are positive parameters

that determine the recipe of the BZ reaction,  $\nabla^2$  is the Laplacian operator, and the parameter  $\phi$  represents the rate of photochemical bromide production due to irradiation. The Euler method was used for numerical simulations, with  $dx = 0.15$  and  $dt = 0.001$ , and the parameters were  $f = 0.5$ ,  $q = 1 \times 10^{-3}$ ,  $\varepsilon = 4 \times 10^{-3}$ , and  $\varepsilon' = 4 \times 10^{-4}$ .

## REFERENCES

- <sup>1</sup>M. Vaduganathan, G. A. Mensah, J. Varieur Turco, V. Fuster, and G. A. Roth, "The global burden of cardiovascular diseases and risk," *J. Am. Coll. Cardiol.* **80**(25), 2361–2371 (2022).
- <sup>2</sup>S. S. Virani, A. Alonso, H. J. Aparicio, E. J. Benjamin, M. S. Bittencourt, C. W. Callaway, A. P. Carson, A. M. Chamberlain, S. Cheng, F. N. Delling, M. S. V. Elkind, K. R. Evenson, J. F. Ferguson, D. K. Gupta, S. S. Khan, B. M. Kissela, K. L. Knutson, C. D. Lee, T. T. Lewis, J. Liu, M. S. Loop, P. L. Lutsey, J. Ma, J. Mackey, S. S. Martin, D. B. Matchar, M. E. Mussolino, S. D. Navaneethan, A. M. Perak, G. A. Roth, Z. Samad, G. M. Satou, E. B. Schroeder, S. H. Shah, C. M. Shay, A. Stokes, L. B. VanWagner, N.-Y. Wang, and C. W. Tsao, "Heart disease and stroke statistics—2021 update," *Circulation* **143**(8), e254–e743 (2021).
- <sup>3</sup>C. X. Wong, A. Brown, D. H. Lau, S. S. Chugh, C. M. Albert, J. M. Kalman, and P. Sanders, "Epidemiology of sudden cardiac death: Global and regional perspectives," *Heart Lung Circ.* **28**(1), 6–14 (2018).
- <sup>4</sup>Z.-J. Zheng, J. B. Croft, W. H. Giles, and G. A. Mensah, "Sudden cardiac death in the United States, 1989 to 1998," *Circulation* **104**(18), 2158–2163 (2001).
- <sup>5</sup>D. J. Dossdall, V. G. Fast, and R. E. Ideker, "Mechanisms of defibrillation," *Annu. Rev. Biomed. Eng.* **12**, 233–258 (2010).
- <sup>6</sup>J. L. Prevost and F. Batelli, "Sur quelques aspects des décharges électriques sur le coeur des mammifères," *CR Seances Acad. Sci.* **129**, 1267–1268 (1899).
- <sup>7</sup>I. R. Efimov, Y. Cheng, D. R. Van Wagoner, T. Mazgalev, and P. J. Tchou, "Virtual electrode-induced phase singularity: A basic mechanism of defibrillation failure," *Circ. Res.* **82**(8), 918–925 (1998).
- <sup>8</sup>N. DeTat, A. Kaboudian, and F. H. Fenton, "Terminating spiral waves with a single designed stimulus: Teleportation as the mechanism for defibrillation," *Proc. Natl. Acad. Sci. U. S. A.* **119**(24), e2117568119 (2022).
- <sup>9</sup>T. Amemiya, S. Kádár, P. Kettunen, and K. Showalter, "Spiral wave formation in three-dimensional excitable media," *Phys. Rev. Lett.* **77**(15), 3244–3247 (1996).
- <sup>10</sup>V. K. Vanag and I. R. Epstein, "Segmented spiral waves in a reaction-diffusion system," *Proc. Natl. Acad. Sci. U. S. A.* **100**(25), 14635–14638 (2003).
- <sup>11</sup>A. S. Adabag, R. V. Luepker, V. L. Roger, and B. J. Gersh, "Sudden cardiac death: Epidemiology and risk factors," *Nat. Rev. Cardiol.* **7**(4), 216–225 (2010).
- <sup>12</sup>J. M. Davidenko, A. V. Pertsov, R. Salomonsz, W. Baxter, and J. Jalife, "Stationary and drifting spiral waves of excitation in isolated cardiac muscle," *Nature* **355**(6358), 349–351 (1992).
- <sup>13</sup>A. T. Winfree, "Electrical instability in cardiac muscle: Phase singularities and rotors," *J. Theor. Biol.* **138**(3), 353–405 (1989).
- <sup>14</sup>E. M. Cherry and F. H. Fenton, "Visualization of spiral and scroll waves in simulated and experimental cardiac tissue," *New J. Phys.* **10**(12), 125016 (2008).
- <sup>15</sup>F. H. Fenton, S. Luther, E. M. Cherry, N. F. Otani, V. Krinsky, A. Pumir, E. Bodenschatz, and R. F. Gilmour, Jr., "Termination of atrial fibrillation using pulsed low-energy far-field stimulation," *Circulation* **120**, 467–476 (2009).
- <sup>16</sup>R. A. Gray, A. M. Pertsov, and J. Jalife, "Spatial and temporal organization during cardiac fibrillation," *Nature* **392**(6671), 75–78 (1998).
- <sup>17</sup>S. Luther, F. H. Fenton, B. G. Kornreich, A. Squires, P. Bittihn, D. Hornung, M. Zabel, J. Flanders, A. Gladuli, L. Campoy, E. M. Cherry, G. Luther, G. Hasenfuss, V. I. Krinsky, A. Pumir, R. F. Gilmour, Jr., and E. Bodenschatz, "Low-energy control of electrical turbulence in the heart," *Nature* **475**(7355), 235–239 (2011).
- <sup>18</sup>W. Li, A. H. Janardhan, V. V. Fedorov, Q. Sha, R. B. Schuessler, and I. R. Efimov, "Low-energy multistage atrial defibrillation therapy terminates atrial fibrillation with less energy than a single shock," *Circ. Arrhythmia Electrophysiol.* **4**(6), 917–925 (2011).
- <sup>19</sup>A. T. Winfree, *When Time Breaks Down: The Three-Dimensional Dynamics of Electrochemical Waves and Cardiac Arrhythmias* (Princeton University Press, 1987).



- <sup>20</sup>A. T. Winfree and S. H. Strogatz, "Singular filaments organize chemical waves in three dimensions: I. Geometrically simple waves," *Physica D* **8**, 35–49 (1983).
- <sup>21</sup>V. I. Krinsky, V. N. Biktashev, and A. M. Pertsov, "Autowave approaches to cessation of reentrant arrhythmias," *Ann. N. Y. Acad. Sci.* **591**(1), 232–246 (1990).
- <sup>22</sup>J. P. Keener, "The topology of defibrillation," *J. Theor. Biol.* **230**(4), 459–473 (2004).
- <sup>23</sup>C. D. Marcotte and R. O. Grigoriev, "Dynamical mechanism of atrial fibrillation: A topological approach," *Chaos* **27**(9), 093936 (2017).
- <sup>24</sup>A. M. Pertsov, M. Wellner, V. Vinson, and J. Jalife, "Topological constraint on scroll wave pinning," *Phys. Rev. Lett.* **84**(12), 2738–2741 (2000).
- <sup>25</sup>A. F. Taylor, "Mechanism and phenomenology of an oscillating chemical reaction," *Prog. React. Kinet. Mech.* **27**(4), 247–326 (2002).
- <sup>26</sup>R. Toth and A. F. Taylor, "The tris(2,2'-bipyridyl)ruthenium-catalysed Belousov-Zhabotinsky reaction," *Prog. React. Kinet. Mech.* **31**(2), 59–115 (2006).
- <sup>27</sup>D. Yengi, M. R. Tinsley, and K. Showalter, "Autonomous cycling between excitatory and inhibitory coupling in photosensitive chemical oscillators," *Chaos* **28**(4) (2018).
- <sup>28</sup>A. J. Steele, M. Tinsley, and K. Showalter, "Collective behavior of stabilized reaction-diffusion waves," *Chaos* **18**(2) (2008).
- <sup>29</sup>P. Jung, A. Cornell-Bell, F. Moss, S. Kadar, J. Wang, and K. Showalter, "Noise sustained waves in subexcitable media: From chemical waves to brain waves," *Chaos* **8**(3), 567–575 (1998).
- <sup>30</sup>T. Yamaguchi, L. Kuhnert, Z. Nagy-Ungvarai, S. C. Mueller, and B. Hess, "Gel systems for the Belousov-Zhabotinskii reaction," *J. Phys. Chem.* **95**(15), 5831–5837 (1991).
- <sup>31</sup>T. Amemiya, P. Kettunen, S. Kádár, T. Yamaguchi, and K. Showalter, "Formation and evolution of scroll waves in photosensitive excitable media," *Chaos* **8**(4), 872–878 (1998).
- <sup>32</sup>T. Sakurai, E. Mihaliuk, F. Chirila, and K. Showalter, "Design and control of wave propagation patterns in excitable media," *Science* **296**(5575), 2009–2012 (2002).
- <sup>33</sup>S. Kádár, T. Amemiya, and K. Showalter, "Reaction mechanism for light sensitivity of the Ru(bpy)<sub>3</sub><sup>2+</sup> catalyzed Belousov-Zhabotinsky reaction," *J. Phys. Chem. A* **101**(44), 8200–8206 (1997).
- <sup>34</sup>Y. Mori, Y. Nakamichi, T. Sekiguchi, N. Okazaki, T. Matsumura, and I. Hanazaki, "Photo-induction of chemical oscillation in the Belousov-Zhabotinsky reaction under the flow condition," *Chem. Phys. Lett.* **211**(4), 421–424 (1993).
- <sup>35</sup>R. J. Field and R. M. Noyes, "Oscillations in chemical systems. IV. Limit cycle behavior in a model of a real chemical reaction," *J. Chem. Phys.* **60**(5), 1877–1884 (1974).
- <sup>36</sup>J. Tyson and P. C. Fife, "Target patterns in a realistic model of the Belousov-Zhabotinskii reaction," *J. Chem. Phys.* **73**(5), 2224–2237 (1980).
- <sup>37</sup>A. M. Pertsov, J. M. Davidenko, R. Salomonsz, W. T. Baxter, and J. Jalife, "Spiral waves of excitation underlie reentrant activity in isolated cardiac muscle," *Circ. Res.* **72**(3), 631–650 (1993).
- <sup>38</sup>D. W. Frazier, P. D. Wolf, J. M. Wharton, A. S. Tang, W. M. Smith, and R. E. Ideker, "Stimulus-induced critical point. Mechanism for electrical initiation of reentry in normal canine myocardium," *J. Clin. Invest.* **83**(3), 1039–1052 (1989).
- <sup>39</sup>R. Tóth, V. Gáspár, A. Belmonte, M. C. O'Connell, A. Taylor, and S. K. Scott, "Wave initiation in the ferroin-catalysed Belousov-Zhabotinsky reaction with visible light," *Phys. Chem. Chem. Phys.* **2**(3), 413–416 (2000).
- <sup>40</sup>N. Chattapakorn, I. Banville, R. A. Gray, and R. E. Ideker, "Effects of shock strengths on ventricular defibrillation failure," *Cardiovasc. Res.* **61**(1), 39–44 (2004).
- <sup>41</sup>I. R. Efimov, Y. Cheng, Y. Yamanouchi, and P. J. Tchou, "Direct evidence of the role of virtual electrode-induced phase singularity in success and failure of defibrillation," *J. Cardiovasc. Electrophysiol.* **11**(8), 861–868 (2000).
- <sup>42</sup>D. Barkley, "Euclidean symmetry and the dynamics of rotating spiral waves," *Phys. Rev. Lett.* **72**(1), 164–167 (1994).
- <sup>43</sup>A. T. Winfree, "Electrical turbulence in three-dimensional heart muscle," *Science* **266**(5187), 1003–1006 (1994).
- <sup>44</sup>F. Fenton and A. Karma, "Vortex dynamics in three-dimensional continuous myocardium with fiber rotation: Filament instability and fibrillation," *Chaos* **8**(1), 20–47 (1998).
- <sup>45</sup>W. Liu, J. L. Han, J. Tomek, G. Bub, and E. Entcheva, "Simultaneous wide-field voltage and dye-free optical mapping quantifies electromechanical waves in human induced pluripotent stem cell-derived cardiomyocytes," *ACS Photonics* **10**(4), 1070–1083 (2023).
- <sup>46</sup>T. Amemiya, T. Ohmori, M. Nakaiwa, and T. Yamaguchi, "Two-parameter stochastic resonance in a model of the photosensitive Belousov-Zhabotinsky reaction in a flow system," *J. Phys. Chem. A* **102**(24), 4537–4542 (1998).
- <sup>47</sup>T. Ichino, K. Fujio, M. Matsushita, and S. Nakata, "Wave propagation in the photosensitive Belousov-Zhabotinsky reaction across an asymmetric gap," *J. Phys. Chem. A* **113**(11), 2304–2308 (2009).
- <sup>48</sup>T. R. Chigwada, P. Parmananda, and K. Showalter, "Resonance pacemakers in excitable media," *Phys. Rev. Lett.* **96**(24), 244101 (2006).